Synthesis and Characterization of Unsymmetrically β-Substituted Porphyrin Liquid Crystals: Influence of the Chemical Structure on the Mesophase Ordering

Antoni Segade, Mercè Castella, Francisco López-Calahorra, and Dolores Velasco*

Departament de Química Orgànica, Universitat de Barcelona, Martí i Franquès 1-11, E-08028 Barcelona, Catalunya, Spain

Received May 4, 2005. Revised Manuscript Received July 15, 2005

The present study addresses the synthesis and characterization of a series of columnar liquid crystal compounds based on the natural porphyrin hemin. These compounds, which have different alkyl side chains (Alk = butyl, octyl, dodecyl, and hexadecyl) and either free base (M = 2H) or metalated (M = Zn, Cu) porphyrin cores, display hexagonal columnar mesophases over wide temperature ranges that cover room temperature. In the octyl, dodecyl, and hexadecyl free base compounds, the formation of a low-temperature mesophase (Col_{h1}) on cooling from a high-temperature mesophase (Col_{h2}) is marked by a slow transition. Furthermore, the X-ray diffraction pattern of the Col_{h1} mesophase indicates that intracolumnar noncovalent associations of three porphyrin molecules might be formed. As suggested by computer molecular modeling combined with the experimental data, the mobility of the propionic ester chains attached to the porphyrin core and the influence of metalation on porphyrin−porphyrin interactions may account for the mesophase structures encountered in the reported compounds.

1. Introduction

Liquid crystalline systems combine the ordered structure of a crystal phase with the molecular mobility of an isotropic (liquid) phase. This mobility allows liquid crystal mesophases to self-correct structural defects and to show response to external factors such as electrical or magnetic fields. Efforts have been made to efficiently use liquid crystals in electronic devices,[1] addressing such properties as electrical or photoconductivity,[2−4] light emission,[5] ferroelectricity,[6] or information storage.[7]

Thermotropic discotic liquid crystals are an important subclass of the liquid crystal family.[8] First discovered by Chandrasekhar and co-workers,[9] they consist of an aromatic core surrounded by several attached alkyl chains. These molecules can form highly ordered columnar mesophases, lending a highly anisotropic quality to the material properties. Triphenylenes,[10,11] phthalocyanines,[12−15] or hexa-*peri*-hexabenzocoronenes[16−18] have been extensively used as aromatic cores, but also porphyrins[19−30] and related structures[31−34]

* Corresponding author. Telephone: + 34 93 4039260. Fax: + 34 93 3397878. E-mail: dvelasco@ub.edu.

(1) O'Neill, M.; Kelly, S. M. *Adv. Mater.* **2003**, *15*, 1135.
(2) Eichhorn, H. *J. Porphyrins Phthalocyanines* **2000**, *4*, 88.
(3) Bushby, R. J.; Lozman, O. R. *Curr. Opin. Solid State. Mater. Sci.* **2002**, *6*, 569.
(4) Warman, J. M.; van de Craats, A. M. *Mol. Cryst. Liq. Cryst.* **2003**, *396*, 41.
(5) Hassheider, T.; Benning, S. A.; Kitzerow, H.-S.; Achard, M.-F.; Bock, H. *Angew. Chem., Int. Ed.* **2001**, *40*, 2060.
(6) Hird, M.; Goodby, J. W.; Hindmarsh, P.; Lewis, R. A.; Toyne, K. J. *Ferroelectrics* **2002**, *276*, 219.
(7) Liu, C.-Y.; Pan, H.-Y.; Fox, M. A.; Bard, A. J. *Chem. Mater.* **1997**, *9*, 1422.
(8) Bushby, R. J.; Lozman, O. R. *Curr. Opin. Colloid Interface Sci.* **2002**, *7*, 343, and references therein.
(9) Chandrasekhar, S.; Sadashiva, B. K.; Suresh, K. A. *Pramana* **1977**, *9*, 471.
(10) Kumar, S.; Naidu, J. J. *Liq. Cryst.* **2002**, *29*, 899.
(11) Bushby, R. J.; Boden, N.; Kilner, C. A.; Lozman, O. R.; Lu, Z.; Liu, Q.; Thornton-Pett, M. A. *J. Mater. Chem.* **2003**, *13*, 470.
(12) Ban, K.; Nishizawa, K.; Ohta, K.; van de Craats, A. M.; Warman, J. M.; Yamamoto, I.; Shirai, H. *J. Mater. Chem.* **2001**, *11*, 321.
(13) Hatsusaka, K.; Kimura, M.; Ohta, K. *Bull. Chem. Soc. Jpn.* **2003**, *76*, 781.
(14) Binnemans, K.; Sleven, J.; De Feyter, S.; De Schryver, F. C.; Donnio, B.; Guillon, D. *Chem. Mater.* **2003**, *15*, 3930.
(15) Gearba, R. I.; Bondar, A. I.; Goderis, B.; Bras, W.; Ivanov, D. A. *Chem. Mater.* **2005**, *17*, 2585.
(16) Brand, J. D.; Kübel, C.; Ito, S.; Müllen, K. *Chem. Mater.* **2000**, *12*, 1638.
(17) Pisula, K.; Kastler, M.; Wasserfallen, D.; Pakula, T.; Müllen, K. *J. Am. Chem. Soc.* **2004**, *126*, 8074.
(18) Liu, C.; Fechtenkötter, A.; Watson, M. D.; Müllen, K.; Bard, A. J. *Chem. Mater.* **2003**, *15*, 124.
(19) For a review, see: Chou, J.-H.; Kosal, M. E.; Nalwa, H. S.; Rakow, N. A.; Suslick, K. S. *The Porphyrin Handbook*; Kadish, K. M., Smith, K. M., Guilard, R., Eds.; Academic Press: New York, 2000; Vol. 6, p 43.
(20) Goodby, J. W.; Robinson, P. S.; Teo, B.-K.; Cladis, P. E. *Mol. Cryst. Liq. Cryst.* **1980**, *56*, 303.
(21) Gregg, B. A.; Fox, M. A.; Bard, A. J. *J. Am. Chem. Soc.* **1989**, *111*, 3024.
(22) Shimizu, Y.; Miya, M.; Nagata, A.; Ohta, K.; Yamamoto, I.; Kusabyashi, S. *Liq. Cryst.* **1993**, *14*, 795.
(23) Wang, Q. M., Bruce, D. W. *Angew. Chem., Int. Ed. Engl.* **1997**, *36*, 150.
(24) Ohta, K.; Yamaguchi, N.; Yamamoto, I. *J. Mater. Chem.* **1998**, *8*, 2637.
(25) Patel, B. M.; Suslick, K. S. *J. Am. Chem. Soc.* **1998**, *120*, 11802.
(26) Ohta, K.; Ando, M.; Yamamoto, I. *J. Porphyrins Phthalocyanines* **1999**, *3*, 249.
(27) Miwa, H.; Kobayashi, N.; Ban, K.; Ohta, K. *Bull. Chem. Soc. Jpn.* **1999**, *72*, 2719.
(28) Paganuzzi, V.; Guatteri, P.; Riccardi, P.; Sacchelli, T.; Barberá, J.; Costa, M.; Dalcanale, E. *Eur. J. Org. Chem.* **1999**, 1527.
(29) Nakai, T.; Ban, K.; Ohta, K.; Kimura, K. *J. Mater. Chem.* **2002**, *12*, 844.
(30) Liu, W.; Shi, Y.; Shi, T.; Liu, G.; Liu, Y.; Wang, C.; Zhang, W. *Liq. Cryst.* **2003**, *30*, 1255.
(31) Lelj, F.; Morelli, G.; Ricciardi, G.; Roviello, A.; Sirigu, A. *Liq. Cryst.* **1992**, *12*, 941.
(32) Eichhorn, S. H.; Bruce, D. W.; Guillon, D.; Gallani, J.-L.; Fischer, T.; Stumpe, J.; Geue, T. *J. Mater. Chem.* **2001**, *11*, 1576.

10.1021/cm050945l CCC: $30.25
Published on Web 09/27/2005

have found wide applicability. The substitution pattern on the porphyrin ring, usually octa-*β*-substitution, 5,15-di- or 5,10,15,20-tetra-*meso*-substitution, permits fine-tuning of the degree of order of the mesophase, from the only orientational order of the discotic nematic mesophase (N_D) to the high two-dimensional positional order of the columnar mesophase (Col_x).[23,24] Metalation of the porphyrin core can also be essential for the mesomorphic behavior of the compound as well as for the display of properties such as magnetism or luminescence.[35−37]

In recent years, our research group has pursued the preparation of porphyrin liquid crystals and the study of their applicable properties.[38,39] Porphyrin macrocycles are usually obtained by the condensation of conveniently functionalized pyrroles or dipyrromethanes with aldehydes.[40,41] However, these methods have serious drawbacks, including moderate yields, difficult purifications, and sensitivity to functional groups. To avoid such drawbacks in the synthesis of porphyrin liquid crystals, we turned to hemin (ferriprotoporphyrin IX chloride, **1**), a commercially available product in which the porphyrin ring is already formed. A short step and good yielding functionalization of this product could provide an effective method to prepare porphyrin derivatives with liquid crystalline properties.

This paper describes the synthesis and characterization of a series of columnar liquid crystals obtained from hemin.[39] Furthermore, they are an example of unsymmetrically *β*-substituted liquid crystal porphyrins, a structural feature that has an important influence on the ordering of the molecules within the mesophase.

2. Experimental Section

Materials and Methods. All reactions involving porphyrins were carried out with light protection using aluminum foil. Hemin was purchased from Fluka. All reagents were used as received. CH_2Cl_2 and Et_3N were distilled from CaH_2; THF was distilled from sodium/benzophenone; DMF was dried by storing it over activated 4 Å molecular sieves under an argon atmosphere. Flash chromatography was carried out over silica gel (SDS, 230−240 mesh). Compounds were characterized by ^{1}H NMR, ^{13}C NMR, and MS and by CHN analysis for the final compounds. POM observation was performed using a Nikon Eclipse polarizing microscope equipped with a Linkam THMS 600 hot stage and a Linkam CI 93 programmable temperature controller. DSC were recorded using a Mettler-Toledo DSC821 module at a scan rate of 10 °C min^{-1} under nitrogen flow. X-ray diffractograms were recorded using either an image plate with Kiesig geometry, a Debye−Scherrer Inel CPS-120, or a Siemens D-500 with Bragg-Bentano theta/2theta geometry. All equipment was fitted with temperature-controlling devices. AM1 semiempirical calculations were performed on a PC computer with the GaussView 3.0/Gaussian 03 Revision B.04 software,[42] using the default optimization parameters (Berny optimization algorithm without initial generation of force constants).

13,17-Bis(2-carboxyethyl)-2,7,12,18-tetramethylporphyrin-3,8-diacrylic Acid (4). Tetraester **3** (100 mg, 142 *μ*mol) was dissolved in 22 mL of DME and 24 mL of aqueous KOH (0.7 N). After the solution was stirred at room temperature for 5 days, DME was evaporated and the resulting aqueous solution was brought to pH = 5 by adding acetic acid. The precipitated solid was washed with water, centrifuged, and dried. Yield: 92% (85 mg, 131 *μ*mol). Due to its insolubility in the most common solvents, NMR spectra could not be recorded. MS (MALDI-TOF, DHB): 651.4 (MH^+).

General Procedure for the Dialkylation of 5-Methoxyresorcinol: 3,5-Didodecyloxyanisole (8). 5-Methoxyresorcinol (**5**) (535 mg, 3.82 mmol), anhydrous potassium carbonate (2.17 g, 15.69 mmol), dodecyl bromide (2.96 g, 11.86 mmol), and a catalytic amount of KI were dissolved in 15 mL of anhydrous DMF. The mixture was gently refluxed under a nitrogen atmosphere for 17 h overnight. After cooling, the mixture was poured over 100 mL of ice/water and 100 mL of AcOEt. The organic layer was washed with 2 × 100 mL of water and 100 mL of aqueous saturated NaCl, dried over anhydrous magnesium sulfate, and evaporated. The residue was purified by flash chromatography (hexane:CH_2Cl_2 4:1). Yield: 94% (1.72 g, 3.60 mmol). ^{1}H NMR ($CDCl_3$, 300 MHz): *δ* 6.07 (s, H_2, H_4, H_6, 3H), 3.90 (t, $-OCH_2C_{11}H_{23}$, 4H), 3.76 (s, $-OCH_3$, 3H), 1.74−0.88 (m, $-OCH_2C_{11}H_{23}$, 46H), ^{13}C NMR ($CDCl_3$, 75 MHz): *δ* 161.3 (C_1), 160.9 (C_3, C_5), 93.7 (C_2, C_6), 93.2 (C_4), 68.0 ($-OCH_2C_{11}H_{23}$), 55.3 ($-OCH_3$), 32.0−14.2 ($-OCH_2C_{11}H_{23}$). MS (CI−NH_3, 70 eV): 478 (MH^+, 100%).

General Procedure for the Selective Cleavage of Aryl Methyl Ethers: 3,5-Didodecyloxyphenol (12). Under a nitrogen atmosphere, NaH (3.37 g, 49 mmol, 60% suspension in mineral oil) was suspended in 75 mL of anhydrous DMF and the resulting mixture was cooled at 0 °C. Ethanethiol (8.0 mL, 108 mmol) was then slowly added and when hydrogen bubbling had ceased, the solution was left to reach room temperature. A solution of compound **8** (1.51 g, 3.17 mmol) in 20 mL of dry DMF was added via cannula and the mixture was gently refluxed for 1.5 h. After cooling, 200 mL of water was added and the solution was extracted with 2 × 200 mL of AcOEt. The combined organic layers were washed with 3 × 100 mL of saturated aqueous NaCl and dried over anhydrous magnesium sulfate, and the solvent was evaporated. The residue was purified by flash chromatography (CH_2Cl_2:hexane 2:1). Yield: 81% (1.18 g, 2.55 mmol). ^{1}H NMR ($CDCl_3$, 300 MHz): *δ* 6.06 (t, H_4, 1H), 5.99 (d, H_2, H_6, 2H), 4.96 (s, −O*H*, 1H), 3.88 (t, $-OCH_2C_{11}H_{23}$, 4H), 1.72−0.88 (m, $-OCH_2C_{11}H_{23}$,

(33) Sessler, J. L.; Callaway, W.; Dudek, S. P.; Date, R. W.; Lynch, V.; Bruce, D. W. *Chem. Commun.* **2003**, 2422.
(34) Qi, M.-H.; Liu, G.-F. *J. Mater. Chem.* **2003**, *13*, 2479.
(35) *Metallomesogens*; Serrano, J. L., Ed.; VCH: Weinheim, Germany, 1996.
(36) Giroud-Godquin, A. M. *Handbook of Liquid Crystals*; Demus, D., Ed.; Wiley-VCH: Weinheim, Germany, 1998; Vol. 2B, p 901.
(37) Donnio, B.; Guillon, D.; Deschenaux, R.; Bruce, D. W. *Comprehensive Coordination Chemistry II*; McCleverty, J. A., Meyer, T. J., Eds.; Elsevier Ltd.: Oxford, UK, 2004; Vol. 7, p 357.
(38) Castella, M.; López-Calahorra, F.; Velasco, D.; Finkelmann, H. *Liq. Cryst.* **2002**, *29*, 559.
(39) Preliminary communication: Castella, M.; López-Calahorra, F.; Velasco, D.; Finkelmann, H. *Chem. Commun.* **2002**, 2348.
(40) Smith, K. M. *J. Porphyrins Phthalocyanines* **2000**, *4*, 319.
(41) Shanmugathasan, S.; Edwards, C.; Boyle, R. W. *Tetrahedron* **2000**, *56*, 1025.
(42) Frisch, M. J.; Trucks, G. W.; Schlegel, H. B.; Scuseria, G. E.; Robb, M. A.; Cheeseman, J. R.; Montgomery, J. A., Jr.; Vreven, T.; Kudin, K. N.; Burant, J. C.; Millam, J. M.; Iyengar, S. S.; Tomasi, J.; Barone, V.; Mennucci, B.; Cossi, M.; Scalmani, G.; Rega, N.; Petersson, G. A.; Nakatsuji, H.; Hada, M.; Ehara, M.; Toyota, K.; Fukuda, R.; Hasegawa, J.; Ishida, M.; Nakajima, T.; Honda, Y.; Kitao, O.; Nakai, H.; Klene, M.; Li, X.; Knox, J. E.; Hratchian, H. P.; Cross, J. B.; Adamo, C.; Jaramillo, J.; Gomperts, R.; Stratmann, R. E.; Yazyev, O.; Austin, A. J.; Cammi, R.; Pomelli, C.; Ochterski, J. W.; Ayala, P. Y.; Morokuma, K.; Voth, G. A.; Salvador, P.; Dannenberg, J. J.; Zakrzewski, V. G.; Dapprich, S.; Daniels, A. D.; Strain, M. C.; Farkas, O.; Malick, D. K.; Rabuck, A. D.; Raghavachari, K.; Foresman, J. B.; Ortiz, J. V.; Cui, Q.; Baboul, A. G.; Clifford, S.; Cioslowski, J.; Stefanov, B. B.; Liu, G.; Liashenko, A.; Piskorz, P.; Komaromi, I.; Martin, R. L.; Fox, D. J.; Keith, T.; Al-Laham, M. A.; Peng, C. Y.; Nanayakkara, A.; Challacombe, M.; Gill, P. M. W.; Johnson, B.; Chen, W.; Wong, M. W.; Gonzalez, C.; Pople, J. A. *Gaussian 03*, Revision B.04; Gaussian, Inc.: Pittsburgh, 2003.

4H). ^{13}C NMR ($CDCl_3$, 75 MHz): δ 161.0 (C_3, C_5), 157.1 (C_1), 94.5 (C_2, C_6), 94.1 (C_4), 68.1 ($-OCH_2C_{11}H_{23}$), 32.0−14.2 ($-CH_2C_{11}H_{23}$). MS (CI−NH_3, 70 eV): 464 (MH^+, 100%), 463 (M^+, 1%).

General Procedure for the Tetraesterification of Compound 4 with Phenols 10−13: 3,5-Didodecyloxyphenyl 13,17-Bis[(2-(3,5-didodecyloxy)phenyloxycarbonyl)-ethyl]-2,7,12,18-tetramethylporphyrin-3,8-diacrylate (16a). Tetraacid **4** (250 mg, 385 μmol) was suspended in 12 mL of anhydrous THF under an argon atmosphere. Thionyl chloride (1.7 mL, 23.3 mmol) was added, immediately producing a bright green solution. After the solution was stirred at room temperature for 1 h, the solvent was evaporated using a water vacuum pump, and the residue was dried for 1 h in a vacuum desiccator with P_2O_5. The resulting green solid was redissolved in 25 mL of anhydrous CH_2Cl_2 in an argon atmosphere, and after the solution cooled to 0 °C, a solution of phenol **12** (500 mg, 1.08 mmol), DMAP (11 mg, 90 μmol), and Et_3N (0.38 mL, 2.73 mmol) in 10 mL of anhydrous CH_2Cl_2 was added via cannula. The porphyrin solution rapidly became red, and after it reached room temperature, it was stirred for 3 h. After that time, the solvent was evaporated and the residue was dried for 1 h using an oil pump. After the solution was redissolved in 25 mL of anhydrous CH_2Cl_2 under an inert atmosphere, another solution of phenol **12** (353 mg, 763 μmol) and DCC (545 mg, 2.64 mmol) in 15 mL of anhydrous CH_2Cl_2 was added via cannula. The solution was further stirred for 14 h overnight. The solvent was distilled and the resulting residue was purified by flash chromatography (hexane:AcOEt 50:3). The isolated product was then washed three times with MeOH to remove the phenol that had coeluted. Yield: 36% (340 mg, 140 μmol). ^{1}H NMR ($CDCl_3$, 300 MHz): δ 10.25, 10.15, 10.13 (3s, *meso*-H, 4H), 9.57, 9.55 (2d, $-CH$═CHCOO−, 2H), 7.37, 7.36 (2d, −CH═C*H*COO−, 2H), 6.63 (d, H_2, H_6, 4H), 6.51 (t, H_4, 2H), 6.08 (t, $H_{4'}$, 2H), 5.63 (d, $H_{2'}$, $H_{6'}$, 4H), 4.49 (m, $-CH_2CH_2COO-$, 4H), 4.07 (t, $-OCH_2C_{11}H_{23}$, 8H), 3.90−3.69 (4s, ring-CH_3, 12H), 3.45 (m, $-CH_2CH_2COO-$, 4H), 3.17 (m, $-OCH_2C_{11}H_{23}$, 8H), 1.88−0.91 (m, $-OCH_2C_{11}H_{23}$, 184 H), −4.42 (bs, −N*H*, 2H). ^{13}C NMR ($CDCl_3$, 75 MHz): δ 171.4 ($-CH_2CH_2COO-$), 165.7 (−CH═CH*C*OO−), 160.9, 160.2 (C_3, $C_{3'}$, C_5, $C_{5'}$), 156.0−136.0 (C_α, C_β), 152.6, 151.8 (C_1, $C_{1'}$), 138.8 ($-CH$═CHCOO−), 121.3 (−CH═*C*HCOO−), 100.8, 100.0 (C_2, $C_{2'}$, C_6, $C_{6'}$), 99.4, 99.1 (C_4, $C_{4'}$), 97.9, 97.8 (C_{meso}), 68.4, 67.6 ($-OCH_2C_{11}H_{23}$), 36.6 ($-CH_2CH_2$-COO−), 31.9−14.1 ($-OCH_2C_{11}H_{23}$), 22.0 ($-CH_2CH_2COO-$), 13.6−11.8 (ring-CH_3). MS (MALDI-TOF, DHB): 2429.1 (M^+, 100%). CHN Analysis: $C_{156}H_{242}N_4O_{16}$. Calcd (%): C, 77.12; H, 10.04; N, 2.31. Found (%): C, 76.68; H, 9.96; N, 2.21.

General Procedure for the Metalation of Porphyrin Tetraesters: Compound 16b. A mixture of tetraester **16a** (24 mg, 9.9 μmol) and $Zn(AcO)_2 \cdot 2H_2O$ (12 mg, 55 μmol) in 2 mL of dry DMF was heated to 115 °C for 30 min. After cooling, the reaction mixture was diluted with 15 mL of CH_2Cl_2, washed in 3 × 15 mL of water, dried over anhydrous sodium sulfate, and evaporated. The residue was purified by flash chromatography (hexane:AcOEt 8:2). Yield: 92% (23 mg, 9.2 μmol). ^{1}H NMR ($CDCl_3$, 300 MHz): δ 9.46, 9.33, 9.08 (3s, *meso*-H, 4H), 9.25, 9.18 (2d, $-CH$═CHCOO−, 2H), 7.22, 7.17 (2d, −CH═C*H*COO−, 2H), 6.68 (d, H_2, H_6, 4H), 6.50 (t, H_4, 2H), 5.94 (t, $H_{4'}$, 2H), 5.41 (d, $H_{2'}$, $H_{6'}$, 4H), 4.38, 4.28 (2m, $-CH_2CH_2COO-$, 4H), 4.04 (t, $-OCH_2C_{11}H_{23}$, 8H), 3.71−3.41 (4s, ring-CH_3, 12H), 3.19, 3.11 (2m, $-CH_2CH_2COO-$, 4H), 3.05 (m, $-OCH_2C_{11}H_{23}$, 8H), 1.51−0.90 (m, $-CH_2C_{11}H_{23}$, 184 H). ^{13}C NMR ($CDCl_3$, 75 MHz): δ 171.4 ($-CH_2CH_2COO-$), 166.0 (−CH═CH*C*OO−), 160.9, 160.1 (C_3, $C_{3'}$, C_5, $C_{5'}$), 156.7−131.9 (C_α, C_β), 152.7, 151.7 (C_1, $C_{1'}$), 139.0, 138.2 ($-CH$═CHCOO−), 120.2 (−CH═*C*HCOO−), 100.9, 100.0 (C_2, $C_{2'}$, C_6, $C_{6'}$), 99.6, 98.9 (C_4, $C_{4'}$), 97.9 (C_{meso}), 68.4, 67.6 ($-OCH_2C_{11}H_{23}$), 36.6−14.1 ($-OCH_2C_{11}H_{23}$), 21.8 ($-CH_2CH_2COO-$), 13.7−11.8 (ring-CH_3). MS (MALDI-TOF, DHB/THF): 2489.8 (^{64}Zn). CHN Analysis: $C_{156}H_{240}N_4O_{16}Zn$. Calcd (%): C, 75.16; H, 9.70; N, 2.25. Found (%): C, 74.82; H, 9.77; N, 2.04.

Scheme 1. Synthesis of the Hemin-Based Liquid Crystal Compounds[a]

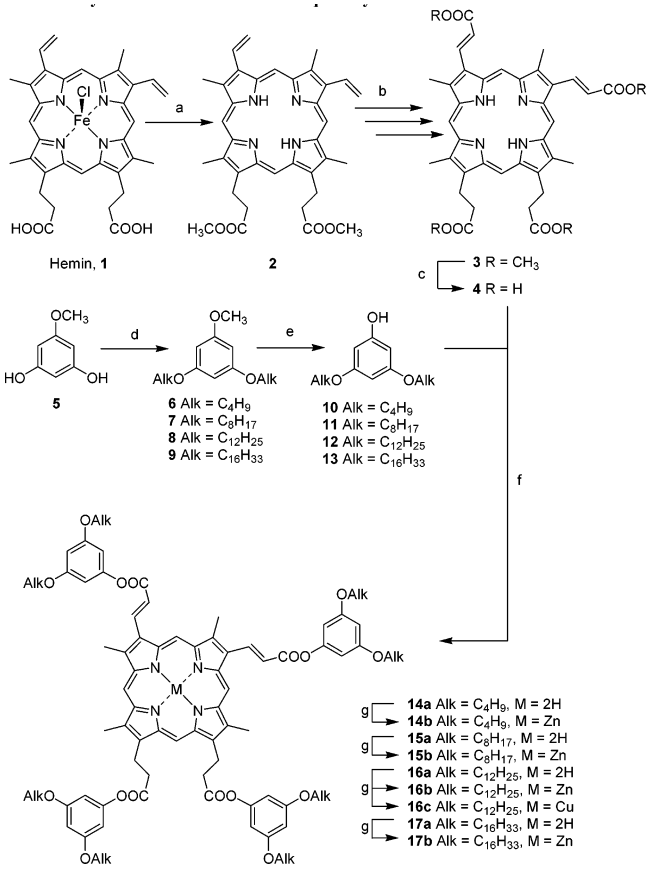

[a] Reagents and conditions: (a) $FeSO_4 \cdot 7H_2O$, HCl(g), MeOH, CH_2Cl_2, r.t., 85%; (b) ref 44, 3 steps, 83% overall; (c) KOH, DME/H_2O, r.t., 92%; (d) AlkBr, K_2CO_3, KI, DMF, reflux, 57−94%; (e) EtSH, NaH, DMF, reflux, 70−90%; (f) *1*. $SOCl_2$, THF, r.t., *2*. **10**−**13**, Et_3N, DMAP, CH_2Cl_2, 0 °C to r.t., *3*. **10**−**13**, DCC, DMAP, CH_2Cl_2, r.t., 32−40%; (g) $M(AcO)_2$, DMF, 115 °C, 89−98%.

3. Synthesis

Compounds **14**−**17** were synthesized following the route depicted in Scheme 1. Demetalation and esterification of hemin[40,43] furnished protoporphyrin IX dimethyl ester (**2**), which was then transformed into tetraester **3** using the reaction sequence developed by Kahl and co-workers.[44] The transformations on the porphyrin core were accomplished with the nearly quantitative hydrolysis of the four methyl esters.

The phenyl units containing the alkyl side chains were synthesized starting from 5-methoxyresorcinol (**5**), by the etherification of the hydroxyl groups using the corresponding alkyl bromides. Subsequent selective cleavage of the aryl methyl ether using EtSNa in DMF[45] furnished 3,5-dialkyloxyphenols **10**−**13** with good yields (70−90%).

As tetraacid **4** proved to be insoluble in the most common organic solvents, direct esterification of the phenols could not be performed. Instead, tetraacid **4** was first transformed into the acyl chloride by treatment with thionyl chloride. Reaction with the phenol in basic

(43) Grinstein, M. *J. Biol. Chem.* **1947**, *167*, 515.
(44) Kahl, S. B.; Schaeck, J. J.; Koo, M.-S. *J. Org. Chem.* **1997**, *62*, 1875.
(45) Feutrill, G. I.; Mirrington, R. N. *Tetrahedron Lett.* **1970**, *16*, 1327.

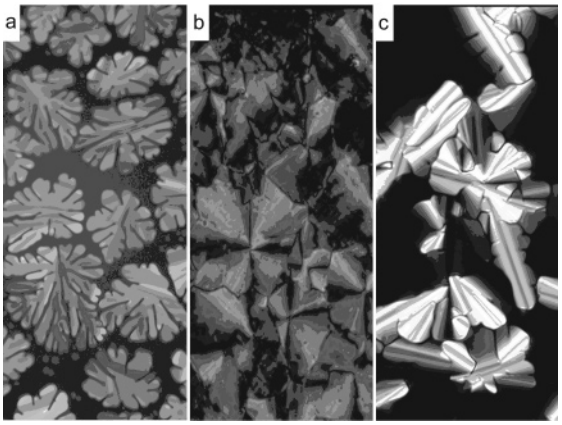

Figure 1. POM textures, cooling from the isotropic state. (a) Compound **14a** at 115 °C; (b) compound **16a** at 110 °C; (c) compound **16c** at 160 °C.

media yielded a mixture of mono-, di-, and triester compounds, based on MALDI-TOF mass spectrometry. Further esterification using DCC as the coupling reagent provided the free base compounds **14**−**17a**. Yields following the three combined steps ranged from 32% to 40%. Tetraester free base compounds were metalated either with Zn (**14**−**17b**) or with Cu (**16c**) by reaction with its corresponding metal (II) acetate in hot DMF. In addition to consistent spectral data, all free base and metalated tetraester compounds provided satisfactory CHN analyses.

4. Characterization of the Mesomorphic Behavior

Polarized Optical Microscopy (POM). When initially observed at room temperature, all the compounds were sticky, birefringent, and highly viscous, with the characteristic aspect of a mesophase. Upon heating, mesophases became less viscous until the clearing point was reached. Some general trends were observed: (a) the shorter the side alkyl chains, the higher the clearing point; (b) metalated analogues (**14**−**17b**, **16c** compounds) were thermally more stable than their parent free base compounds (**14**−**17a**).

Upon cooling to room temperature (ca. 20 °C), textures generally associated with columnar mesophases were obtained (see pictures in Figure 1), but no crystallization was observed. Exceptions were compounds **14b** and **15b**, which did not recover any birefringence nor did they exhibit any type of texture. TLC analysis demonstrated that decomposition of the compounds had occurred during the melting process. This is not very surprising, given the high temperatures reached during isotropization.

When the free base compounds **15a**, **16a**, and **17a** were subjected to annealing at room temperature for several hours, textures were still characteristic of columnar mesophases, although they were less birefringent. However, during a second heating run, a sudden recovery of birefringence was observed around 50−60 °C.

Differential Scanning Calorimetry (DSC). DSC events for each of the compounds studied are summarized in Table 1. Clearing points were consistent with those observed in the POM experiments, while decomposition of compounds **14b** and **15b** was also confirmed, since no transitions were detected after the first heating run.

Upon cooling, different processes were observed. For compounds **16a** and **17a**, a small peak at ca. 40 °C appeared

Table 1. DSC Characterization of the Synthesized Liquid Crystal Compounds[a,b]

compound	transition	temperature/°C	ΔH/kJ mol^{-1}
14a	g → Col_{h1}	13	
	Col_{h1} → I	193	0.9
14b	g → Col_{h1}	11[c]	
	Col_{h1} → dec.	303[d]	*d*
15a	g → Col_{h1}	−10	
	Col_{h1} → Col_{h2}	ca. 50[d]	*d*
	Col_{h2} → I	168	3.7
15b	g → Col_{h2}	−5	
	Col_{h2} → dec.	244[e]	13.7
16a	g → Col_{h1}	−31	
	Col_{h1} → Col_{h2}[f]	51[f]	1.1[f]
	Col_{h1} → Col_{h2}[g]	65[g]	23.0[g]
	Col_{h2} → I	139	4.9
16b	g → Col_{h2}	−25	
	Col_{h2} → I	192	6.4
16c	g → Col_{h2}	−31	
	Col_{h2} → I	174	4.1
17a	Cr → Col_{h1}	22	115.3
	Col_{h1} → Col_{h2}	53	3.3[f]
	Col_{h2} → I	108	4.2
17b	Cr → Col_{h2}	23	115.3
	Col_{ha2} → I	153	6.0

[a] g = glassy state; Cr = crystal; Col_h = hexagonal columnar mesophase; I = isotropic liquid; dec. = decomposition. [b] Peak and enthalpy values extracted from second heating runs unless noted otherwise. [c] Extracted from a first cooling run starting from 25 °C. [d] Not detected by DSC but detected by POM. [e] Extracted from a first heating run starting from 25 °C. [f] Without previous annealing. [g] After annealing at r.t. for 48 h.

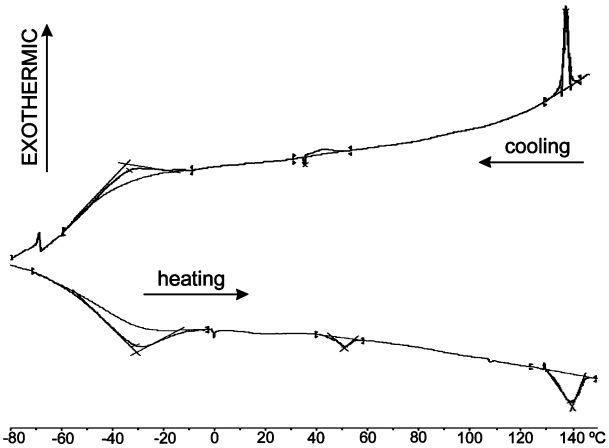

Figure 2. DSC first cooling (upper) and second heating without annealing (lower) of compound **16a**.

(Figure 2). Due to its low enthalpy (1−3 kJ mol^{-1}) and its breadth, it was sometimes detected as a very slight variation in the baseline of the diagram. At lower temperatures, hexadecyl compounds (**17a**, **17b**) exhibited a sharp crystallization peak of 155 kJ mol^{-1}, but no other compounds displayed a similar pattern, revealing instead either round and broad peaks or slope changes in the baseline associated with glass transitions.

In the second heating runs without annealing, transitions were enantiotropic, with temperatures and enthalpies similar to those of the previous cooling run. The small peak at ca. 40 °C moved to a slightly higher temperature, about 50 °C, and clearing temperatures were also increased approximately 5−8 °C. However, when compound **16a** was annealed for several hours at room temperature after cooling, such as in the POM experiments, and then reheated, the small peak at ca. 50 °C was substituted by a much more endothermic peak (23 kJ mol^{-1}) at 65 °C. The isotropization peak stayed

Table 2. XRD Characterization of the Liquid Crystal Mesophases[a]

compound	mesophase	observed spacings/Å[b]	*a*/Å[c]
14a	Col_{h1} (r.t.)	24.0 (10), 12.0 (20), 10.0 (d_3), ca. 6.8 (d_2), 4.4 (alkyl)	27.7
14b	Col_{h1} (r.t.)	23.3 (10), 13.3 (11), 11.6 (20), 10.4 (d_3), 8.9 (21), 4.5 (alkyl)	26.9
15a	Col_{h1} (r.t.)	29.3 (10), 16.7 (11), 14.9 (20), 4.5 (alkyl)	33.8
	Col_{h2} (100 °C)	28.4 (10), 10.5 (21), 4.5 (alkyl), 3.6 (d_1)	32.8
15b	Col_{h2} (r.t.)	28.4 (10), 16.4 (11), 14.2 (20), ca. 11.1 (d_3),[d] 10.7 (21), 4.4 (alkyl), 3.5 (d_1)	32.8
16a	Col_{h1} (r.t.)	33.4 (10), 19.2 (11), 16.8 (20), ca. 10.0 (d_3), 4.5 (alkyl)	38.5
	Col_{h2} (80 °C)	31.3 (10), 11.8 (21), ca. 11.2 (d_3),[d] 4.5 (alkyl), 3.6 (d_1)	36.2
16b	Col_{h2} (r.t.)	31.9 (10), 18.5 (11), 15.8 (20), 12.8 (21), ca. 11.2 (d_3),[d] 4.4 (alkyl), 3.5 (d_1)	36.8
16c	Col_{h2} (r.t.)	31.7 (10), 18.4 (11), 15.9 (20), 12.1 (21), ca. 11.0 (d_3),[d] 10.6 (30), 4.4 (alkyl), 3.5 (d_1)	36.6
17a	Col_{h1} (r.t.)	37.1 (10), 14.0 (21), 4.5 (alkyl)	42.8
	Col_{h2} (85 °C)	34.9 (10), 12.9 (21), 4.5 (alkyl), 3.6 (d_1)	40.3
17b	Col_{h2} (r.t.)	35.0 (10), 20.5 (11), 17.7 (20), 13.3 (21), 11.8 (22), ca. 10.8 (d_3),[d] 4.4 (alkyl), 3.5 (d_1)	40.4

[a] a = lattice parameter; d_1 = intermolecular stacking distance; d_2 = stacking distance between bimolecular associations; d_3 = stacking distance between trimolecular associations. [b] In parentheses, assignment of the (*hk*) indexes or of the structural features. [c] Calculated from the (10) spacings. [d] Very weak.

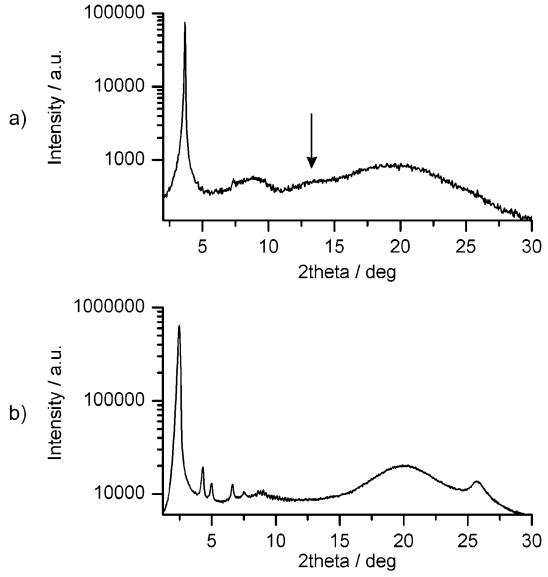

Figure 3. X-ray diffraction patterns: (a) **14a** at 70 °C; (b) **17b** at room temperature. The arrow in (a) indicates the position of the halo at ca. 6.8 Å.

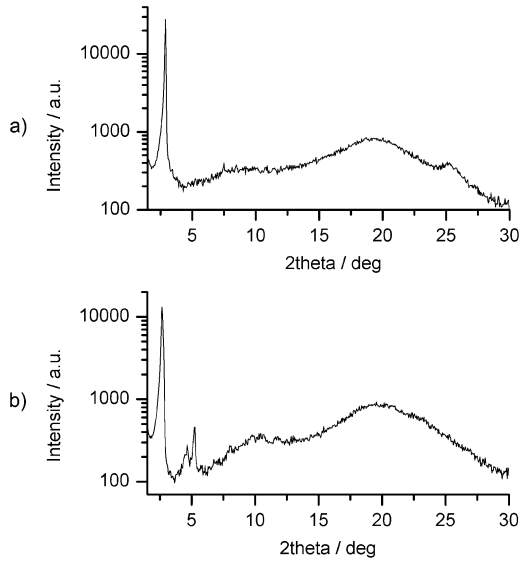

Figure 4. X-ray diffraction patterns of compound **16a**. (a) At 80 °C, the diffraction peak of 3.6 Å and the weak halo of the ca. 11 Å reciprocal distances can be observed. (b) After annealing at room temperature for 48 h, the pattern changes and the peak at 10 Å appears.

invariable. This new transition was linked to the observed POM change in birefringence. Taking the POM results as a base, compounds **15a** and **17a** are also considered likely to present the same DSC behavior.

X-ray Diffraction (XRD). The results obtained from the X-ray experiments at different temperatures and times are presented in Table 2. Hexagonal columnar stacking could be assigned to every recorded pattern: one sharp peak in the low-angle region and minor peaks at $1/\sqrt{3}$, $1/\sqrt{4}$, $1/\sqrt{7}$, $1/\sqrt{9}$,... reciprocal distances of the former were generally detected, and a broad halo at 2θ = ca. 20° belonging to the molten alkyl chains was also detected.

Moreover, certain other signals were also observed, their position, number, and shape dependent upon the studied compound. This additional information permitted us to identify different kinds of organization. In the butyl analogues (**14a** and **14b**), a round signal in the middle-angle region, at a reciprocal distance of ca. 10 Å, was observed (Figure 3a). In addition, a much weaker halo at ca. 6.8 Å was also occasionally detected. This mesophase was noted as Col_{h1}. In the octyl-, dodecyl-, and hexadecyl-metalated compounds (**15**−**17b**, **16c**), a very weak halo at ca. 11 Å, as well as a peak at a 3.5 Å reciprocal distance, was observed (Figure 3b). Another mesophase type, termed Col_{h2}, was assigned to this pattern.

Dodecyl free base compound **16a** exhibited both Col_{h1} and Col_{h2} mesophases in temperature- and time-dependent behavior. After cooling from the isotropic state to 80 °C, the characteristic pattern of the Col_{h2} mesophase emerged, with the broad and weak halo in the middle-angle region and the 3.6 Å reflection (Figure 4a). When the sample was further cooled to room temperature, below the 40 °C DSC transition, the Col_{h2} mesophase pattern remained intact. Taking into account the results of the POM and DSC experiments, a new diffractogram was recorded after annealing at room temperature for 48 h (Figure 4b). The Col_{h1} mesophase was identified, with some minor peaks indicative of hexagonal columnar stacking, with the round signal around 10 Å, and the lack of a peak at 3.6 Å. Reheating the sample to 80 °C again furnished the Col_{h2} diffraction pattern, observed at this temperature during the cooling run. The X-ray studies on the octyl and hexadecyl free base analogues (**15a** and **17a**) were carried out using different equipment than that used for the **16a** studies. Although the signals at 10−11 Å in the middle-angle region were not clearly visible, the same temperature and time dependence was observed, with the changes in the hexagonal columnar spacing, as well as the appearance of the 3.6 Å reflection at high temperatures. It was therefore assumed that compounds **15**−**17a** share this same mesophase behavior.

5. Discussion

Mesogenic Properties. In a previous article we described another hemin-based compound, showing a discotic lamellar (D_L) mesophase.[38] In that compound, two 3,4-didodecyloxyphenyl groups were attached to the porphyrin core through vinyl groups, instead of the 3,5-didodecyloxyphenyl acrylic esters used in the present study. This change in the chemical structure has an important effect on mesophase stability and ordering: the introduction of the ester group and the change in the substitution pattern of the phenyl groups provide a wider temperature range as well as a higher molecular ordering in the mesophase.

One of the most important properties of the compounds reported here is their liquid crystallinity at room temperature, which makes them suitable for several applications.[1,18] Mesophases are stable throughout wide temperature ranges, up to nearly 300 °C for the zinc butyl compound **14b**. It must be noted that decomposition can occur at high temperatures (compounds **14b** and **15b**), but in general these molecules are chemically stable: after heating compound **16a** to 150 °C, beyond its clearing point, for half an hour, its ^{1}H NMR spectrum remained unchanged, demonstrating that neither degradation nor polymerization of the acrylic esters had occurred.

Col_{h2}-Col_{h1} Transition in Free Base Compounds 15−17a. The features observed during the characterization stage demonstrate that the transition from Col_{h2} to Col_{h1} upon cooling is not immediate. This finding is strongly supported by the changes observed in both the DSC curve and the X-ray diffraction pattern when the sample was immediately reheated after cooling, or when it was annealed for several hours at room temperature.

Additional experiments were carried out in order to further evaluate this transition. The same sample used for the preliminary DSC characterization of **16a** was subjected to a cyclic treatment, whereby the sample was heated to isotropization (150 °C), cooled to room temperature (25 °C), and annealed over an increased period of time for each cycle: 5, 10, 20, 40, 60, and 120 min. All cooling runs were identical and the transition at ca. 40 °C was not clearly observed. The mesophase−mesophase transitions observed upon heating following different annealing periods, including the preliminary 48 h (2880 min) cycle, are presented in Figure 5. The DSC peak shows a continuous increase both in temperature and in enthalpy (see inset). After the sample was annealed for 120 min, the conversion to the Col_{h1} mesophase seems to be nearly complete, since no great differences are observed when compared to the 48 h run.

To rule out the possibility that a slow crystallization process is related to this transition, a second DSC heating run was performed after annealing the sample at room temperature for 46 days. Once again, the same peak at 65 °C was obtained, with an enthalpy of 22 kJ mol^{-1}. This value, typical of mesophase−mesophase transitions, is significantly less than that obtained for the crystallization of compound **17a** (115 kJ mol^{-1}). Further evidence supporting the liquid crystalline behavior of **16a** at room temperature is provided by XRD: after cooling the sample from the isotropic state, annealing for a long period (20 days) did not produce any significant change in the diffraction pattern once the Col_{h1} mesophase has been formed.

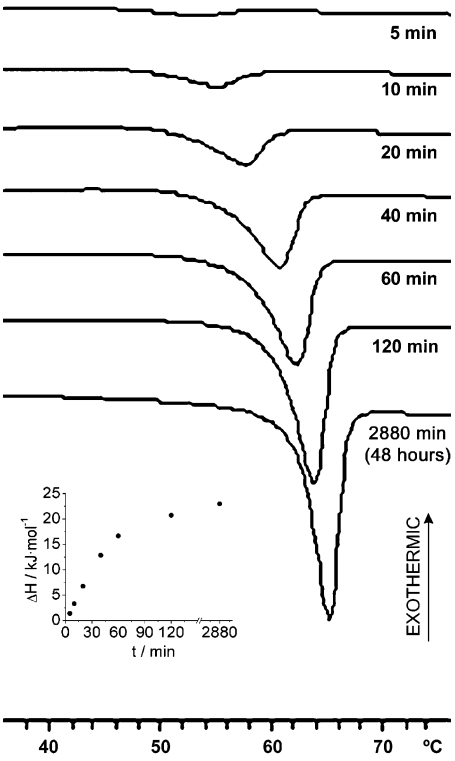

Figure 5. DSC curves on heating compound **16a** after annealing at room temperature for different periods of time. Inset: enthalpies associated with the peaks.

When DSC and XRD results are combined, a more complete description of the mesophase−mesophase transition can be constructed: while the Col_{h2}−Col_{h1} transition occurs very slowly upon cooling, probably due to structural requirements (see below), it occurs rapidly upon heating. This may explain why it was not always visible during the DSC cooling runs. At room temperature just after cooling, the Col_{h2} pattern was still visible via XRD. Annealing is required for mesophase transformation, and its degree of conversion can be monitored through the increase of the peak temperature and enthalpy in heating runs. Molecular mobility in the liquid crystalline phase may permit the existence of "intermediate" phases, distinct from the "pure" Col_{h1} and Col_{h2} states, wherein DSC peak characteristics may correspond to the statistically weighted addition of different states. The more the mesophase state resembles the Col_{h1} organization, the greater would be the energy required for the mesophase−mesophase transition. Indeed, this would be reflected in the increasing enthalpies and temperatures observed in the heating runs following increases to the annealing time periods.

Structural Factors Influencing Mesophase Stability. The structural variety of the different derivatives permits discussion of the influence that alkyl chain length and core metalation may have on mesophase melting and clearing points. Similar studies on porphyrin β-octaesters[28] and bis(phthalocyaninato)lanthanide(III) complexes[14] have been recently published. The results for the compounds reported here are qualitatively consistent with those previous studies.

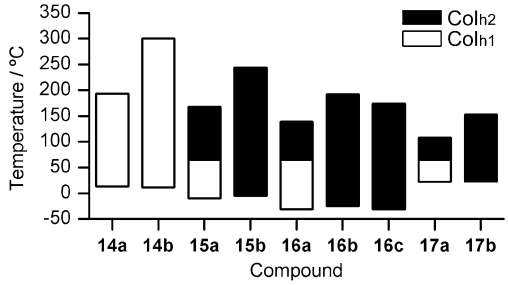

Figure 6. Mesophase temperature ranges of the synthesized liquid crystal compounds.

Compound mesophase ranges are presented in Figure 6. As expected,[14,28,46] alkyl chain length affects the melting point. An intermediate length, the dodecyl one, displays the lowest melting temperature. An increase or decrease in the number of carbon atoms results in an increase of the melting points. Furthermore, a decrease in the clearing point is observed with increasing chain lengths.

Metalation of the porphyrin core has no influence on the melting point: all of the studied compounds sharing the same alkyl chain length melt at the same temperature. In certain other liquid crystal porphyrins, copper metalation has shown no influence on the melting point,[21,26,28,34] while zinc metalation produced different effects, depending on the compound: an increase in the melting point,[21,30] a decrease,[30] or again, no effect.[26]

On the other hand, metalation enhances the thermal stability of mesophases, raising their clearing temperatures by 50−100 °C. The enhanced $\pi-\pi$ interaction between neighboring porphyrins is believed to be responsible for this improvement,[28] as metalation has been shown to increase both the rigidity of the porphyrin rings and their electrostatic attraction.[47] As demonstrated in the dodecyl series, the identity of the metal atom also seems important, as the clearing points $Zn^{2+} > Cu^{2+}$ are consistent with the higher electropositivity of the Zn atom. However, further studies using different alkyl chain lengths and metal atoms are needed to reach definitive conclusions.

Possible Intracolumnar Structure in the Col_{h1} and Col_{h2} Mesophases. The X-ray diffraction patterns exhibited by the various compounds have permitted us to establish a hexagonal columnar organization for all the obtained mesophases. However, the unexpected appearance of additional signals, particularly in the Col_{h1} mesophase, suggests that the molecules possess a supramolecular arrangement slightly different from the usual hexagonal columnar mesophases.

In searching for a possible explanation for these signals, we found that Ohta and co-workers, in their work on cerium(III) multiple-decker porphyrin complexes[27,29] had reported diffraction patterns similar to those of the Col_{h1} mesophase in the present work. It is theoretically possible that the 10 and 6.8 Å distances in our compounds could conform to some kind of three- and two-molecule associations, respectively, as they exhibit nearly triple and double the usual $\pi-\pi$ stacking distance between the single aromatic molecules, 3.5−3.6 Å. Supporting this hypothesis is the relationship between the lattice parameters a and h and the number of molecules per unit cell (Z), expressed as follows: $Z = \rho(VN_A/M)$ whereby V is the volume of the unit cell ($V = \cos(30°)a^2h$ for a hexagonal columnar mesophase), N_A is Avogadro's number, M is the molar mass of the compound, and ρ is its density.[24] If ρ is set between 0.9 and 1.0 g cm^{-3}, typical density values associated with organic compounds, Z values close to 3.0 are obtained (an h value of 10 Å was also used for compounds **15a** and **17a**). Exceptions are the two butyl compounds, which yield lower values, around 2.5.

Perhaps the strongest argument against this hypothesis is that, unlike the covalent attachment of the porphyrin cores to the metal atoms in the cerium(III) complexes, there is no apparent reason for the formation of trimolecular associations. However, previous studies on porphyrins bearing very bulky meso groups,[24] as well as other discotic molecules,[48] have reported bimolecular associations without need of any covalent interaction. Perhaps some sort of side substitution might help to stabilize or to trap these oligomolecular associations.

The columnar arrangement of the Col_{h1} mesophase could be formed by associations of three molecules, with an interassociation distance equal to approximately three $\pi-\pi$ stacking distances, i.e., 3×3.5 Å $= 10.5$ Å. However, as the geometry of the associations would not be well-defined nor their interdistances constant, the resulting XRD signal would be necessarily broad. In addition, a small percentage of consecutive associations with a number of molecules other than three may also exist, as demonstrated by the 6.8 Å halo of compound **14a**. This fact suggests a nonrandom distribution of the associations within the columnar stack.

In the Col_{h2} mesophase, the signal corresponding to the interassociation distance becomes weaker, appearing now a peak of $\pi-\pi$ stacking distance between single molecules. The most likely organization is a hexagonal columnar mesophase with a $\pi-\pi$ stacking distance of 3.5−3.6 Å between single molecules. Although the halo observed at ca. 11 Å would again suggest trimolecular correlations, they would be very weak, indeed nearly nonexistent, with porphyrin associations being largely destroyed.

Effect of the Unsymmetrical Substitutions on Mesophase Ordering. The possible unusual molecular organization within mesophase columnar stacks prompted us to gain further insight into the effects that chemical structures of compounds impose on the liquid crystal behavior: butyl compounds (series **14**) exhibit only the Col_{h1} mesophase; metalated compounds with longer alkyl chains (**15**−**17b**, **16c**) display only the Col_{h2} mesophase; and free base compounds with longer alkyl chains (**15**−**17a**) display both types, depending on temperature. The unsymmetrical β-substitution of the porphyrin core by two acrylic and two propionic esters, in tandem with the influence of metalation on $\pi-\pi$ stacking interactions, may be the principal factors explaining such mesomorphic behavior.

Computer modeling was used to test this hypothesis. The free base analogue (C1 alkyl chains) of our compounds was

(46) Collard, D. M.; Lillya, P. M. *J. Am. Chem. Soc.* **1991**, *113*, 8577.
(47) Hunter, C. A.; Sanders, J. K. M. *J. Am. Chem. Soc.* **1990**, *112*, 5525.
(48) Attias, A.-J.; Cavalli, C.; Donnio, B.; Guillon, D.; Hapiot, P.; Malthête, J. *Chem. Mater.* **2002**, *14*, 375.

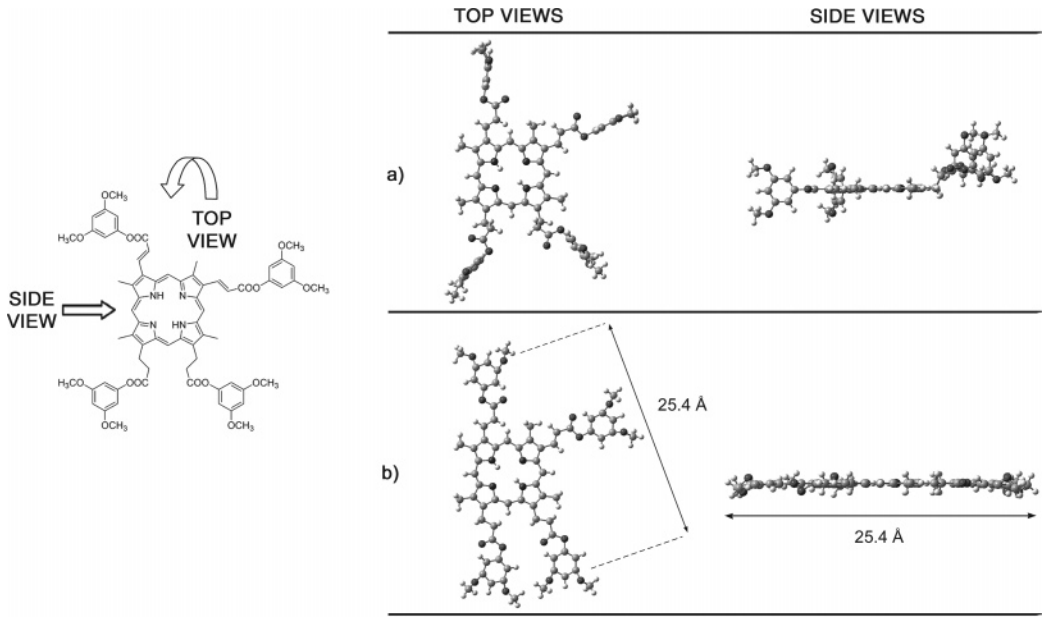

Figure 7. Computer modeled structures (top and side views) of the methyl analogue of liquid crystal compounds **14**−**17**. (a) AM1 optimized geometry; (b) "flat" conformation, with the phenyl rings and the propionic ester chains forced to lie in the porphyrin plane.

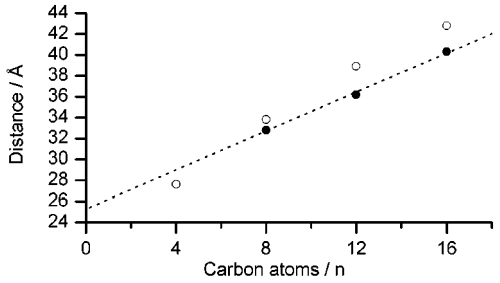

Figure 8. Lattice parameters of the Col_{h1} (empty circles) and the Col_{h2} (filled circles) mesophases of compounds **14**−**17a** versus the corresponding alkyl chain length. The dotted line shows the straight line fitting of the Col_{h2} parameters.

subjected to semiempirical AM1 calculations. In energy-minimized structures (Figure 7a), propionic esters stand out from the plane defined by the porphyrin ring, while the acrylic ester chains are coplanar, which is to be expected as they are conjugated to the central aromatic ring. In a "flat" conformation (Figure 7b), in which the propionic ester chains and the phenyl rings are forced to coexist within the porphyrin plane, the longest core axis, defined by the distance between the two C-4 atoms of the most distant phenyl ester groups, displayed a value of 25.4 Å. Rotation of the phenyl rings from a minimum-energy conformation toward coplanarity with the porphyrin ring seems a plausible option in a real mesophase, the aim being to maximize the $\pi-\pi$ interaction of the aromatic rings between neighboring molecules.

A plot of the lattice parameters of free base compounds versus the length of side alkyl chains is presented in Figure 8. As can be seen, the three Col_{h2} lattice parameters fall below the Col_{h1} parameters for the same compounds, indicating tighter molecular packing. Moreover, the three Col_{h2} parameters reasonably fit along a straight line. Assuming that discotic molecules are formed by a rigid aromatic core surrounded by flexible side chains, the lattice parameter can be divided into a constant contribution, representing the diameter of the aromatic core, and a variable contribution of alkyl chains. Both are obtained from the intercept and the slope of the line. In the present study, an intercept of 25.3 Å and a slope of 0.93 Å (C atom)$^{-1}$ were obtained. This latter value represents approximately 75% of the real distance *per atom* for an alkyl chain in an all-trans conformation, while the former nearly matches the "flat" conformation distance of the computer-modeled analogue. One possibility is that the intracolumnar structure of the Col_{h2} mesophase is formed by the stacking of single molecules in a "flat" conformation, with their mean position centered at the columnar axis. In the Col_{h1} mesophase, an intracolumnar arrangement of trimolecular stacks would be less homogeneous, slightly off-center from the columnar axis. Such an arrangement would produce a columnar structure with a higher cell parameter, but also with a higher intercolumnar order.

Based on these results, the following structures for the two mesophases included in this study seem most plausible. In the Col_{h1} mesophase, molecules would tend toward a structure resembling the AM1 minimum-energy conformation. The propionic ester chains would stand out of the plane defined by both the porphyrin ring and the acrylic esters of the molecule and would invade the planar space of neighboring molecules. Such an intrusion would preclude molecular rotation around the columnar axis, and in addition, the propionate chain conformations would act as a type of "clamp", holding a neighboring ring close to its own porphyrin ring and giving rise to intracolumnar molecular associations. The most stable association, based on geometrical and energetical relationships not fully understood at the present time, would be comprised of three molecules, with their propionate chains mutually holding the neighboring molecules. The intracolumnar arrangement would be based on trimolecular associations, with a stacking distance of approximately 10 Å. In contrast, molecules in the Col_{h2} mesophase would primarily attain a "flat" conformation, with the trimolecular associations proving almost nonexistent.

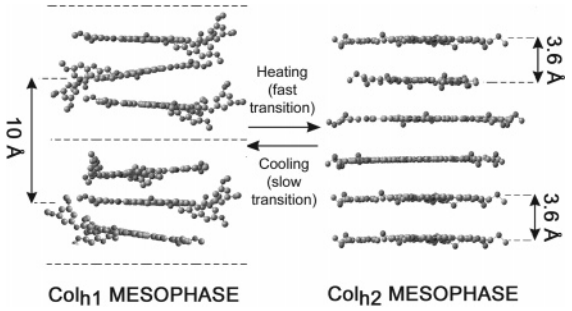

Figure 9. Schematic model for the proposed mesophase structures observed in compounds **15**−**17a** (side alkyl chains omitted for clarity).

Molecular rotation could occur, with the 3.5−3.6 Å peak corresponding to the molecule−molecule stacking then visible in the X-ray diffractogram.

Building upon the hypothesis regarding mesophase structure, the behavior of these studied compounds might best be explained in terms of conformation stabilization. The $\pi-\pi$ interaction between porphyrins seems the most promising source of stabilization since a "flat" conformation permits much better $\pi-\pi$ stacking than the minimum-energy conformation. At this point it should be noted, however, that the side alkyl chain length exerts more than a negligible influence since neither butyl compound follows the same mesophase behavior when compared to their longer chain analogues, but rather displays only the Col$_{h1}$ mesophase.

Thus, in octyl-, dodecyl-, and hexadecyl-metalated compounds (**15**−**17b**, **16c**) such "flat" conformations might be stabilized by improved $\pi-\pi$ intermolecular interactions, whereby the Col$_{h2}$ structure would be visible throughout the whole mesophase range. Previous studies report an enthalpy up to 48 kJ mol^{-1} for zinc porphyrin−zinc porphyrin interactions.[49] On the other hand, there are no clear values for free base porphyrin interactions, although they are likely to be much lower.[47] As the $\pi-\pi$ interaction alone would not be strong enough to stabilize the "flat" conformation, an additional driving force would be needed. This second factor could be temperature, explaining the temperature- and time-dependent behavior of compounds **15**−**17a**. As schematized in Figure 9, at low temperatures a "flat" conformation would not be stabilized, with molecules tending toward the most energy-stable geometry. Here, the propionic ester chains would stand out from the porphyrin plane, forming the trimolecular associations (Col$_{h1}$ mesophase). When the temperature is raised, however, the conformational mobility of the molecules increases and a "flat" conformation is readily attainable, leading to the Col$_{h2}$ mesophase. Upon cooling again, propionic ester chains, now exhibiting lower degrees of conformational freedom, would gravitate toward a lower energy conformation, leading to the appearance of the Col$_{h1}$ mesophase. The transition would occur slowly this time, however, indeed, several hours judging by DSC, since re-accommodation of a single molecule would suggest the corresponding displacement of several neighboring molecules, as well as the partial breaking of porphyrin−porphyrin interactions, until the entire system finally managed to settle into its most stable structure, with the stacking of oligomolecular, noncovalent associations.

6. Conclusions

The present study describes a family of columnar liquid crystals based on hemin, prepared in a few synthetic steps, with general good yield. These synthesized compounds exhibit hexagonal columnar mesophases over wide ranges of temperatures. This study also addresses the potential influences of side chain length and metalation on mesophase thermal stability: side chain length primarily affects melting points, while metalation affects clearing points.

The different mesophases observed for the study compounds might best be explained by the presence of a small mobile part within the discotic molecular core. This structural feature, in tandem with the fine-tuning of other intermolecular interactions, may lead to a conformational flexibility that is transported to the bulk system, thereby altering the molecular structure between and within the columnar stacks.

Acknowledgment. Financial support from the Ministerio de Ciencia y Tecnología (Project BQU 2001-3673) is gratefully acknowledged. A. Segade is the recipient of a doctoral fellowship from the Departament d'Universitats, Recerca i Societat de la Informació (DURSI, Generalitat de Catalunya).

Supporting Information Available: ^{1}H NMR, ^{13}C NMR, MS data, and CHN analyses of the new synthesized compounds (PDF) and Cartesian coordinates for the structures presented in Figure 7 (XYZ files). This material is available free of charge via the Internet at http://pubs.acs.org.

CM050945L

(49) Hunter, C. A.; Meah, M. N.; Sanders, J. K. M. *J. Am. Chem. Soc.* **1990**, *112*, 5773.